



CHALMERS
UNIVERSITY OF TECHNOLOGY

Frequency tuning behaviour of terahertz quantum cascade lasers revealed by a laser beating scheme

Downloaded from: <https://research.chalmers.se>, 2024-04-26 22:57 UTC

Citation for the original published paper (version of record):

GUAN, W., LIAO, X., LI, Z. et al (2021). Frequency tuning behaviour of terahertz quantum cascade lasers revealed by a laser beating scheme. Optics Express, 29(14): 21269-21279. <http://dx.doi.org/10.1364/OE.427326>

N.B. When citing this work, cite the original published paper.

Frequency tuning behaviour of terahertz quantum cascade lasers revealed by a laser beating scheme

WEN GUAN,^{1,2} XIAOYU LIAO,^{1,3} ZIPING LI,¹  WENJIAN WAN,¹
KANG ZHOU,^{1,3} YIRAN ZHAO,^{1,3} CHENJIE WANG,^{1,3} XUHONG MA,^{1,3}
SHUMIN WANG,^{1,4} J. C. CAO,^{1,3} DONG XU,^{1,5} JUNWEN ZHANG,⁶ 
NAN CHI,⁶  AND HUA LI^{1,3,*} 

¹Key Laboratory of Terahertz Solid State Technology, Shanghai Institute of Microsystem and Information Technology, Chinese Academy of Sciences, 865 Changning Road, Shanghai 200050, China

²School of Information Science and Technology, ShanghaiTech University, 393 Middle Huaxia Road, Shanghai 201210, China

³Center of Materials Science and Optoelectronics Engineering, University of Chinese Academy of Sciences, Beijing 100049, China

⁴Department of Microtechnology and Nanoscience, Chalmers University of Technology, 41296 Gothenburg, Sweden

⁵SIMIC Advanced Micro Semiconductors Co., Ltd., 888 2nd West Huanhu Street, Pudong, Shanghai 201306, China

⁶School of Information Science and Technology, Fudan University, Shanghai 200433, China

*hua.li@mail.sim.ac.cn

Abstract: In the terahertz frequency range, the commercialized spectrometers, such as the Fourier transform infrared and time domain spectroscopies, show spectral resolutions between a hundred megahertz and a few gigahertz. Therefore, the high precision frequency tuning ability of terahertz lasers cannot be revealed by these traditional spectroscopic techniques. In this work, we demonstrate a laser beating experiment to investigate the frequency tuning characteristics of terahertz quantum cascade lasers (QCLs) induced by temperature or drive current. Two terahertz QCLs emitting around 4.2 THz with identical active regions and laser dimensions (150 μm wide and 6 mm long) are employed in the beating experiment. One laser is operated as a frequency comb and the other one is driven at a lower current to emit a single frequency. To measure the beating signal, the single mode laser is used as a fast detector (laser self-detection). The laser beating scheme allows the high precision measurement of the frequency tuning of the single mode terahertz QCL. The experimental results show that in the investigated temperature and current ranges, the frequency tuning coefficients of the terahertz QCL are 6.1 MHz/0.1 K (temperature tuning) and 2.7 MHz/mA (current tuning) that cannot be revealed by a traditional terahertz spectrometer. The laser beating technique shows potential abilities in high precision linewidth measurements of narrow absorption lines and multi-channel terahertz communications.

© 2021 Optical Society of America under the terms of the [OSA Open Access Publishing Agreement](#)

1. Introduction

Recently, the spectroscopy has attracted increasing interests due to its wide applications in fundamental science, biological diagnosis, security, etc. Especially, in the terahertz frequency range, spectroscopic applications show prominent advantages because a large amount of fingerprints (characteristic absorption lines) of various substances in gas, solid, liquid phases are located in this frequency range between 0.1 and 10 THz [1–3].

The commercialized Fourier transform infrared (FTIR) and time domain spectroscopies (TDS) have been widely used for spectral measurements in the terahertz frequency range [4–6]. Both

terahertz spectrometers have their own advantages, for instance, the FTIR uses an incoherent lamp as a source and it is featured by the ultra-broad spectral coverage from the visible to terahertz frequency range; the TDS can perform high dynamic range spectral measurements (>40 dB) due to its coherent detection nature in the frequency range between hundred GHz and several THz. Nevertheless, neither FTIR or TDS is capable of high spectral resolution measurements. Most of FTIR spectrometers can work with the highest spectral resolution of GHz level and some spectrometers equipped with extremely long arms of the interferometers can reach a resolution of ~100 MHz but the long scanning time is required [7]. Although the TDS can work with much higher dynamic range, its spectral resolution is also limited in the GHz level. Apart from the above-mentioned two terahertz spectrometers, the terahertz dual-comb spectroscopy shows unique advantages in fast data acquisition without a need of any moving part in the system and potentially high spectral resolution. Different from FTIR and TDS, the dual-comb technique [8–11] employs two frequency combs with slightly different repetition frequencies. The multi-heterodyne down-converted spectra can be detected using a fast terahertz detector and then recorded using a spectrum analyzer [12–16]. Although the dual-comb spectroscopy shows outstanding features, it is an indirect technique for the spectral measurement because what we directly obtained are microwave spectra. Therefore, a link between the microwave and optical spectra should be first determined to finally obtain the spectral information in the terahertz frequency range. Alternatively, another direct technique employing tunable terahertz lasers is promising for the terahertz spectroscopy.

The electrically-pumped semiconductor-based terahertz quantum cascade laser (QCL) with high output power [17,18], high far-field beam quality [19], broad frequency coverage from 1.2 to 5.6 THz [20,21], and high operation temperature of 250 K [22], is an ideal candidate to generate tunable terahertz radiations for spectroscopic applications. On the QCL platform, the single mode operation and its tunability have been already demonstrated by implementing different device geometries, such as distributed feedback (DFB) resonators [23], photonic crystal structures [24,25], graded photonic heterostructure resonators [26] and two-section coupled-cavity waveguides [27–29]. In order to achieve a wide frequency tuning range, external cavities, such as a rotational grating mirror [30] or an output coupler combined with a meta-surface QCL [31], have been demonstrated. Up to now, different approaches have been used to investigate the tuning behaviour of terahertz QCLs. For instance, the simplest way to measure the frequency tuning of the lasers can be implemented by using a FTIR. However, its spectral resolution is limited in the GHz level and the intrinsic high precision tuning ability of the lasers cannot be revealed. The other technique to unveil the high precision tuning characteristics of QCLs is based on the beating scheme that is associated with the optical feedback known since early days of the laser technology [32]. Besides unwanted disturbance of the laser operation, this effect was harvested for optical measurements, typically realized by self-mixing and/or optical injection [33–36]. In particular, Consolino *et al.* investigated the emission linewidth and tunability of a QCL by beating it with a femtosecond frequency comb [37]. However, this scheme relies on an external terahertz detector, which increases the complexity of experimental setup. The laser self-detection [13,38] can save the fast terahertz detector and largely simplify the laser beating setup. It is worth mentioning that the laser self-detection is the unique feature of laser beating scheme employing QCLs. In QCLs, the beating of two frequencies will result in the modulation of population inversion, which is then converted into a current modulation. This current modulation can be measured using the QCL itself as a detector due to the fast carrier relaxation time in QCLs [39].

In this work, we propose a laser beating technique based on the laser self-detection to explore the frequency tuning behaviour of terahertz QCLs emitting around 4.2 THz. two terahertz QCLs are employed in this beating system, one of them is operated in single longitudinal mode and the other laser is operated as a frequency comb. The beatings between the two lasers are measured using the single mode laser itself as a fast detector and directly registered on a spectrum analyzer.

Since the beating system can down-convert the frequency from terahertz to microwave, the measurement resolution is significantly improved to 1 Hz. Therefore, the tuning behaviour of the terahertz QCLs by temperature and/or laser drive current can be discovered in a high precision.

2. Laser beating scheme

The laser beating scheme employed in this work is depicted in Fig. 1. One of the lasers, QCL2, is operated in single longitudinal mode. And the other laser, QCL1, is working as a frequency comb. The comb characteristics of QCL1 can be found in [13]. In principle, the two lasers have identical dimensions and similar performances. Both of them can work as frequency combs by selecting suitable conditions, such as the drive current and operation temperature. The single mode operation of QCL2 is simply achieved by decreasing the laser drive current as shown in Fig. 1(a). Figure 1(b) schematically plots the comb lines of QCL1 (red lines) which are equally spaced by the repetition frequency f_{rep} . The dashed line indicates the emission line of QCL2. The beatings between QCL1 and QCL2 can generate different signals in the microwave frequency range. For example, the beat between the line of QCL2 and its right (left) closest line of QCL1 can generate f_1 (f_2); when QCL2 beats with farther lines of QCL1, more radio frequency (RF) lines, e.g., f_3 and f_4 , can be generated. The relations between f_1, f_2, f_3, f_4 , and f_{rep} are summarized in Fig. 1(c). And if we fix the comb lines of QCL1 and tune the frequency of QCL2, the laser beating scheme will allow us to evaluate the frequency tuning coefficient of QCL2.

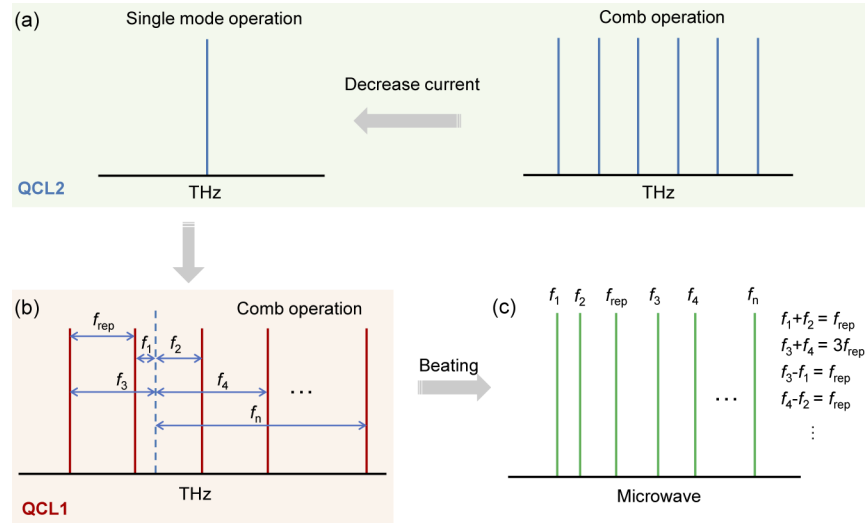


Fig. 1. Schematics of the laser beating processes employed in this work. (a) Single frequency emission of QCL2 achieved by decreasing the laser drive current. The current tuning can force QCL2 to change the operation mode from comb operation to single longitudinal mode operation. (b) Different laser beating processes between QCL1 and QCL2. The red lines are the comb lines of QCL1 and the dashed line represents the single frequency line of QCL2. f_{rep} denotes the repetition frequency of the frequency comb (QCL1) and f_n the beating frequency between the single frequency line (QCL2) and the n -th nearest comb line of QCL1. (c) Down-converted beating signals located in the microwave frequency range. The formulas show the relations of the beating frequencies.

One can say that the beating between two single mode lasers can be also used for the same measurement. Indeed, it is, in principle, possible to use two single mode laser for the beating experiment. However, the beating between two frequencies can only generate one line in the microwave frequency regime. When the beating signal is too weak, it is hard to find the beating

signal especially because the exact frequency values of the two QCLs are unknown. In this work, we beat the single mode QCL with a QCL comb, and multiple beating signals can be generated in the microwave frequency range. Specifically, two lines, i.e., f_1 and f_2 , in the range from 0 to f_{rep} can be definitely found [see Fig. 1(c)]. Therefore, compared to the beating of two single mode lasers, the beating between a single mode laser and a comb makes it more feasible to locate the beating signals in the practical measurements. It is worth noting that in our previous studies, we demonstrated dual-comb operation using the similar experimental setup when the operation conditions for the two QCL combs were firmly fixed. Although the terahertz dual-comb is useful for spectroscopic applications, it is not a good option for the frequency tuning measurement. The reason is the following: when we change the temperature and/or drive current of one comb laser, two frequencies of the comb, i.e., the carrier offset frequency and repetition frequency, will simultaneously change, and therefore, all the comb lines will change accordingly. Because the carrier offset frequency (or the terahertz central frequency) of the comb is unknown, it is difficult to determine the frequency tuning of the terahertz modes. Although one can see the frequency shift in the dual-comb when the conditions of one comb laser is changed, the clear link between the terahertz tuning coefficient and the dual-comb frequency shift cannot be obtained.

Figure 2(a) shows the experimental setup of the frequency tuning measurement. As explained before, two terahertz QCLs, QCL1 and QCL2, are employed in this experiment. The two QCLs are based on a $\text{Al}_{0.25}\text{Ga}_{0.75}\text{As}/\text{GaAs}$ hybrid active region design which combines the bound-to-continuum transitions for the terahertz photon emission and resonant phonon scatterings for the fast depopulation of lower laser state [40]. The QCL wafer was grown using the molecular beam epitaxy on a semi-insulating GaAs (100) substrate, which was then processed into single plasmon waveguide. Finally, 6 mm long laser bars with a ridge width of 150 μm were cleaved and mounted on heat sink coppers for electrical and optical measurements. The light-current-voltage ($L-I-V$) characteristics of QCL1 and QCL2 measured in continuous wave (cw) mode at around 30 K are shown in Figs. 2(b) and 2(c), respectively. Although the two QCLs are nominally identical, the measured laser threshold and optical power values from them are not exactly the same due to the imperfections in material growth, processing, device mounting.

In order to investigate the tuning behaviour of the terahertz QCLs, we operate the two lasers in different ways. QCL1 is operated at 988 mA (see dashed line in Fig. 2(b)) in the frequency comb regime. In the entire measurement, QCL1 is fixed in this situation to generate stable comb lines. On the other hand, QCL2 is tuned by the drive current to work in single mode operation [shaded area in Fig. 2(c)]. The emitted terahertz light from QCL1 is collected and collimated onto the front facet of QCL2 using a pair of parabolic mirrors as shown in Fig. 2(a). The laser self-detection scheme [13,38] is employed to measure the beating signals between QCL1 and QCL2. In this experiment, QCL2 emits single frequency signal and simultaneously acts as a fast terahertz detector to measure the beatings between QCL1 and QCL2. To facilitate the extraction of RF signals from QCL2, a microwave transmission line is mounted close to the laser chip. The extracted RF signals are sent to a Bias-T and then amplified by 30 dB before reaching a spectrum analyzer (Rohde & Schwarz, FSW26).

To verify that the two QCLs can work as expected as what we proposed in Fig. 1, the emission spectra of the two QCLs were first measured using a Fourier transform infrared (FTIR) spectrometer (Bruker, Vertex 80v) with a spectral resolution of 3 GHz. Figure 3(a) shows the measured emission spectra of QCL2 at different drive currents at a fixed temperature of 32 K. It can be seen that as the drive current is beyond 710 mA, the laser is working in multimode. When the current is decreased gradually, the single mode operation can be obtained. Furthermore, as the current is declined to 685 mA, we cannot observe any terahertz signal (see the lowest panel of Fig. 3(a)). Note that this is not meant that QCL2 driven at this current doesn't lase. Actually, due to the signal-to-noise ratio limitation of the FTIR, the weak terahertz signal in this condition cannot be detected. However, employing the laser beating technique, we, in principle, reveal

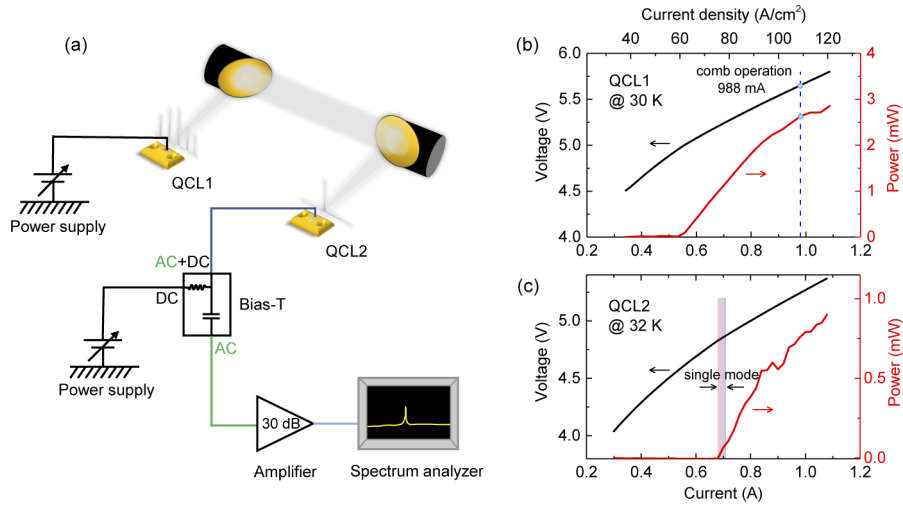


Fig. 2. (a) Experimental setup of the proposed laser beating scheme. QCL1 is operated as a frequency comb while QCL2 is in single mode operation. The Bias-T is used to send the current to QCL2 for laser action and simultaneously extract the beating signals from QCL2. The spectra of the beating signals are finally recorded using a spectrum analyzer with the assistance of a microwave amplifier with a gain of 30 dB. (b) and (c) are measured $L-I-V$ curves of QCL1 at 30 K and QCL2 at 32 K, respectively, in cw mode. All temperature values mentioned in this work refer to the heat sink temperature. The dashed line in (b) indicates the drive current of 988 mA for the comb operation in QCL1. The shaded area close to the laser threshold in (c) depicts the current range for single mode operation of QCL2.

that at an even lower current of 648 mA, the beating signal can be also detected (see Fig. 4(c)), which indirectly proves that QCL2 can emit terahertz photons even at lower drive currents. The emission spectrum of QCL1 driven at 988 mA at 30 K is shown in Fig. 3(b) (black curve). In this fixed condition, QCL1 is working as a frequency comb characterized by a single inter-mode beatnote (f_{rep1}) as shown in Fig. 4(b). For a clear comparison, in Fig. 3(b) the single emission line of QCL2 is also plotted (see the red curve). It can be seen that the two emission spectra have a strong overlap which is crucial for the laser beating experiment.

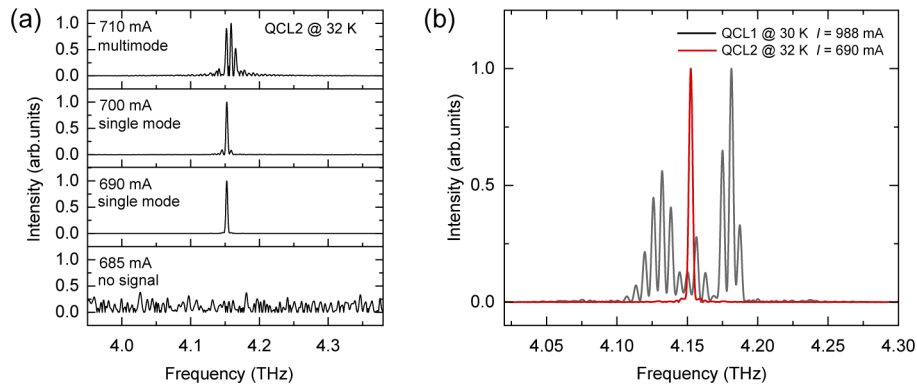


Fig. 3. (a) Emission spectra of QCL2 measured at different drive currents at 32 K. (b) Comb spectrum of QCL1 (black curve) measured at 988 mA at 30 K. The single emission line of QCL2 (red curve) is also shown as a reference.

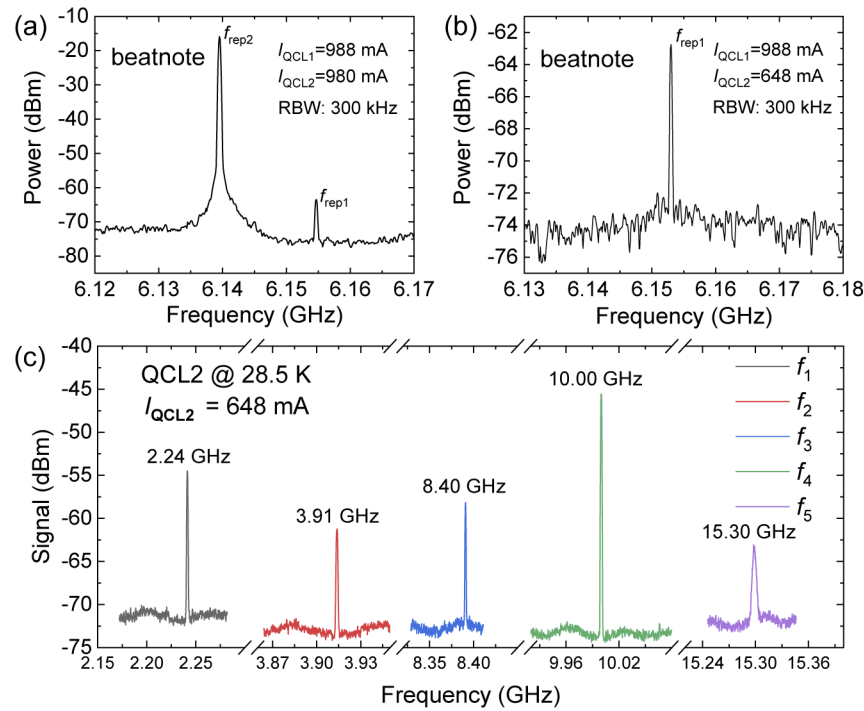


Fig. 4. (a) Inter-mode beatnotes of QCL1 (f_{rep1}) and QCL2 (f_{rep2}) measured with a RBW of 300 kHz when both QCL1 and QCL2 are working as frequency combs. The drive currents of QCL1 and QCL2 are 988 and 980 mA, respectively. (b) Inter-mode beatnote spectrum measured as the drive current of QCL2 is reduced to 648 mA while QCL1 is still electrically pumped at 988 mA. (c) Beating signals between the single frequency line of QCL2 and different comb lines of QCL1. QCL1 is driven at 988 mA at 30 K and QCL2 is driven at 648 mA at 28.5 K.

3. Experimental results and discussion

In Fig. 4, we show the results of the laser beating experiment using QCL2 as a detector. When QCL1 and QCL2 are operated at around 990 mA at 30 K, both of them are capable of comb operation. As shown in Fig. 4(a), the two lasers demonstrate two narrow intermode beatnote frequencies, i.e., f_{rep1} and f_{rep2} , which are the indicators of the frequency comb operation. In Fig. 4(a), the two signals, f_{rep1} and f_{rep2} , show 50 dB difference in power level. This is because we use QCL2 as a detector for RF signal measurements. The intra-cavity detection of f_{rep2} involves less loss than the optical coupling detection of f_{rep1} . As we decrease the drive current of QCL2 to 648 mA, QCL2 switches from comb operation to single mode operation. Therefore, no intermode beat can happen in QCL2 and only f_{rep1} can be observed as shown in Fig. 4(b).

Figure 4(c) shows the beats between the single frequency line of QCL2 and comb lines of QCL1. As depicted in Fig. 1, we can observe five beats, f_1, f_2, \dots, f_5 , ranging from 2.24 to 15.30 GHz. The five beats correspond to the beats between the single line of QCL2 and the five nearest comb lines of QCL1. The relations of the five beats satisfy those formulas expressed in Fig. 1(c). The result shown in Fig. 4(c) experimentally proves that the laser beating scheme can work with our QCLs. Furthermore, it also indicates that the detection bandwidth of the laser beating system can reach at least 15 GHz. In the experiment, the power of a beating signal is determined by several factors, for example, the powers of the two terahertz modes from QCL1 and QCL2, the frequency difference between the two terahertz modes. If the two terahertz modes participating in

the beating process have fixed powers, the power of the beating signal will decrease monotonously with increasing frequency. However, in our experiment, the power of each comb line of QCL1 participating in the beatings varies each time. Therefore, we cannot observe a regular decrease in power with increasing frequency in Fig. 4(c); on the contrary, we can see that f_4 shows even higher power than other beating signals.

After the operation concept is experimentally proved, we can employ the laser beating scheme to investigate the frequency tuning behaviour of the single mode laser (QCL2). Normally, there are two ways to efficiently tune the frequency of semiconductor lasers, i.e., temperature and current. In Fig. 5, we first show the results obtained from the temperature tuning. In this experiment, the current and temperature of QCL1 are fixed at 988 mA and 30 K, respectively; the current of QCL2 is fixed at 648 mA while the temperature is slightly changed. [Visualization 1](#) dynamically displays the spectra of f_2 as the temperature is changed. Figures 5(a), 5(b), and 5(c) show the temperature tuning behaviours of f_1 , f_2 , and f_3 , respectively. It can be seen that as the temperature is decreased, f_1 and f_3 move towards higher frequencies, while f_2 shifts to lower frequencies. The opposite tuning trends can be explained as follows. As shown in Fig. 1(b), f_1 and f_3 are generated from the beatings between the single frequency line of QCL2 and the comb lines of QCL1 on the left hand side of the single frequency line of QCL2. Therefore, when the single frequency line of QCL2 is tuned, f_1 and f_3 show same trend as shown in Figs. 5(a) and 5(c). Regarding f_2 , because f_1 and f_2 satisfy the relation of $f_1 + f_2 = f_{\text{rep}}$ and f_{rep} is a constant, f_2 always shows opposite frequency tuning trend. Note that the frequency tuning range shown in Fig. 5(a) is much narrower than those shown in Figs. 5(b) and 5(c). It is because when the temperature is lower than 27.5 K, f_1 moves into a noisy spectral range (caused by environmental noise and electronic noise of microwave devices used in the measurement) and it cannot be clearly distinguished (see [Visualization 2](#)). However, from Fig. 5(b), the full tuning range of 212 MHz by lowering temperature from 28.9 to 25.3 K can be clearly obtained. When the temperature is lower than 25.3 K, QCL2 no longer maintains single mode operation inferred by appearance of sidemodes; and when the temperature is higher than 28.9 K, the weak signal of QCL2 cannot beat with QCL1 and generate a detectable beating signal f_2 . In the given temperature ranges, the temperature tuning coefficients of 6.5 MHz/0.1 K, 5.9 MHz/0.1 K, and 5.8 MHz/0.1 K can be extracted from Figs. 5(a), 5(b), and 5(c), respectively, which gives an average tuning coefficient of 6.1 MHz/0.1 K. In the laser beating experiment, the comb lines of QCL1 are fixed, therefore, the measured tuning coefficient of 6.1 MHz/0.1 K shows the tuning behaviour of QCL2 induced by temperature.

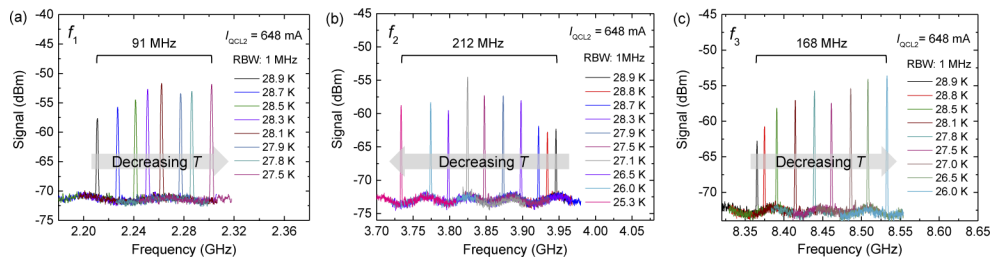


Fig. 5. Temperature tuning characteristics of f_1 (a), f_2 (b), and f_3 (c) measured using the laser beating technique. In this measurement, the drive current and temperature of QCL1 are fixed at 988 mA and 30 K, respectively; the drive current of QCL2 is fixed at 648 mA, while the temperature is decreased from 28.9 to 25.3 K. The grey arrows show the temperature decreasing directions.

Figure 6 shows the frequency tuning behaviour of the laser (QCL2) by changing the drive current. In the current tuning experiment, QCL2 is stabilized at a heat sink temperature of

32 K and the drive current is increased from 680 to 705 mA. Similar to the results shown in Fig. 5, the frequency tuning by drive current can be clearly observed employing the laser beating technique. Furthermore, we see that f_1 and f_3 show same tuning trend as the drive current is increased; while f_2 demonstrates opposite tuning trend. Due to the existence of multiple noisy spectral ranges in lower frequencies, f_1 is strongly affected by strong noises (see Fig. 6(a)). In higher frequencies where f_2 and f_3 are located, clean signals can be obtained. Visualization 3 records the frequency tuning behaviour of f_2 as the drive current is changed. Figures 6(b) and 6(c) show the current tuning coefficients of 2.6 and 2.8 MHz/mA, respectively, which gives an average value of 2.7 MHz/mA. From Figs. 5 and 6, we can find that for each beating signal (f_1 , f_2 , or f_3) the frequency tuning trend with increasing temperature shows opposition tuning trend with increasing drive current. This phenomenon shows good agreements with the results discovered by FTIR measurements, i.e., frequency redshift with temperature vs. blueshift with drive current. Because of this, the relative position between the single frequency line of QCL2 and the two nearest comb lines of QCL1 can be determined. For example, if we look at f_1 in Fig. 5(a), we can see that it moves to lower frequencies when the temperature is increased. Since the frequency redshift of QCLs with temperature is already known, we can deduce that in the terahertz range, the single frequency line of QCL2 is closer to the comb line on its left hand side, as we schematically plot in Fig. 1(b).

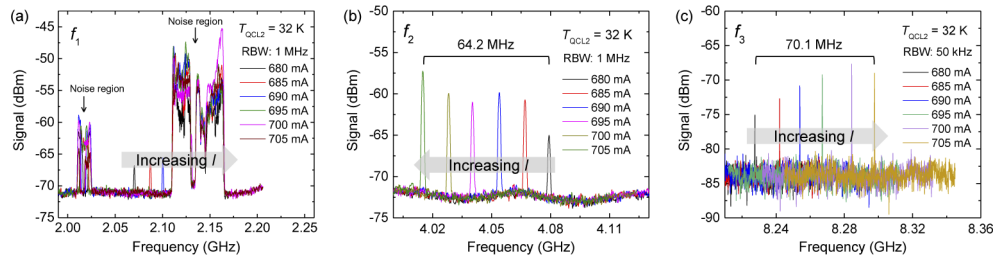


Fig. 6. Drive current tuning characteristics of f_1 (a), f_2 (b), and f_3 (c) measured using the laser beating technique. The drive current and temperature of QCL1 are fixed at 988 mA and 10 K, respectively. The temperature of QCL2 is fixed at 32 K, while the current is varied from 675 to 710 mA. The grey arrows show the current increasing directions.

It can be clearly seen that the measured tuning coefficients for f_1 , f_2 , and f_3 induced by temperature (Fig. 5) or drive current (Fig. 6) are not exactly identical. The small differences among the measured tuning coefficients for f_1 , f_2 , and f_3 are attributed to the measurement uncertainties. Note that in this experiment, no phase locking technique is applied to the lasers. Therefore, the frequency lines are still moving and they are sensitive to the environmental fluctuations, e.g., drive current, temperature, vibration noise, etc. In the measurements, we recorded the spectra of f_1 , f_2 , and f_3 at different times, therefore, the fluctuations finally result in the slight differences among them. One may assume that the other factor, i.e., frequency pulling effect, could bring about the differences in the measured tuning coefficients. Actually, the pulling effect strongly works on the closest frequency line. From Fig. 1(b), we can see that if the pulling effect exist, the single frequency will pull the comb line on its left hand side. If we take the temperature tuning as an example (see Fig. 5), as the temperature is increased, the single mode frequency of QCL2 will move toward the lower frequency (red shift) and then the measured frequency change of f_1 be smaller than that of f_2 . However, the measured temperature tuning coefficients for f_1 and f_2 are 6.5 MHz/0.1 K and 5.9 MHz/0.1 K, respectively, which shows the opposite trend to the expected one. In view of this, we conclude that the frequency pulling effect is not the main reason for the different tuning coefficients measured for f_1 , f_2 , and f_3 . Furthermore, note that in our experiment, the single mode frequency is more than 2 GHz away from the closest

comb line [see Fig. 4(c)]. For the two far-separated frequency lines, the pulling effect cannot contribute to much for the tuning coefficient measurements.

In Figs. 5 and 6, we demonstrate that the laser beating technique can be employed to investigate the frequency tuning characteristics of the terahertz QCLs induced by temperature and drive current. In addition, although the frequency tuning ranges induced by temperature and/or current are narrow due to the limited dynamic ranges of the single mode operation of QCL2, as far as we know the measured frequency tuning coefficients, i.e., 6.1 MHz/0.1K and 2.7 MHz/mA, show the highest spectral precision so far. Furthermore, the compact laser beating setup is capable of real-time measurements of the down-converted spectra without a need of any moving part in the system. The high spectral precision and fast data acquisition time are far beyond the functions of traditional FTIR spectrometers. It has to note that in this work we use a Fabry-Perot (FP) laser (QCL2) to generate single frequency line by lowering its drive current to the threshold. In principle, we can also use a distribute feedback (DFB) laser for study its tuning behaviour in wide dynamic ranges. Because a DFB laser normally lases in a narrow bandwidth due to the grating structures, it is inherently not capable of broadband detection. Therefore, to detect the various beating signals like f_1, f_2, f_3 shown in Figs. 5 and 6, the comb laser (QCL1) rather than the DFB laser should be used as a detector for the multi-heterodyne detection. To experimentally demonstrate its detection capability, in Fig. S1 (see Supplement 1) we show the setup and measured beating signals employing a comb as a fast detector. Two microwave signal at f_1 (f_2) resulted from the beating between the single mode laser and its closest (second closest) comb line is obtained.

Compared to other QCL-based beating systems, the unique feature of the presented beating setup in the current work is its compactness because the laser self-detection is employed and an external fast terahertz detector can be saved. However, because the two QCLs are operated in free running, the frequency precision is still limited. In [41], Mohandas *et al.* demonstrated the exact frequency and phase control of a terahertz QCL emitting at 2 THz by using a locking technique. In that work, the terahertz QCL was phase locked to a stable terahertz signal generated from an all-fiber infrared comb. Once the locking is implemented, the heterodyne linewidth can be reduced to <1 Hz level and the QCL frequency can be tuned in an ultrahigh precision determined only by the microwave synthesizer resolution. Inspired by the work reported in [41], to further improve the measurement precision of our laser beating system, similar locking techniques, in principle, can be implemented. However, the main point is that in our laser system the operation frequency is 4.2 THz which is far beyond the working frequency in [41]. Currently, the terahertz generation techniques based on either electronics (microwave multiplications) or optics (nonlinear crystals or photo-conductive antennas) cannot efficiently work at the high frequency of 4.2 THz, which makes the complete locking of the QCLs rather difficult. This also explains that by employing the free running QCLs, although the tuning coefficients can be measured easily, it is still difficult to precisely obtain the terahertz absolute frequency. However, it is still promising to implement the full phase locking of the QCLs in the future with fast developments of terahertz generation and sensitive detection techniques. Once the QCL is locked with a stable terahertz source generated optically or electrically as we mentioned before, the absolute frequency of the QCL and its current and temperature frequency tuning can be obtained for high precision spectroscopic applications.

Finally, the laser beating technique shows potentials for several practical applications. First of all, it shows potential abilities to measure the line shape of a narrow absorption line. Because the down-converted spectra can be visually recorded using a spectrum analyzer in real-time, we can fast tune the laser frequency by temperature and/or current, and then obtain the intensity at each frequency point. If a narrow absorption line is located in the frequency range of the tunable laser, its line shape (hence the linewidth) can be experimentally determined. On the other hand, the system can be used for terahertz communications (data transmissions). If we modulate the

single mode laser (QCL2), in principle the envelope can be demodulated by QCL1. It also means that the data that are carried by the terahertz light emitted from QCL2 can transmit and then be received by QCL1. More importantly, our experimental results show that we have multiple channels (f_1, f_2, \dots, f_n) to transmit the information. This could be a novel solution for terahertz communications using QCLs.

4. Conclusion

In summary, we have demonstrated a laser beating scheme to investigate the frequency tuning characteristics of terahertz QCLs. In the work, the beating signals between the single frequency line of one QCL and comb lines of the other QCL were detected using the QCL itself as a detector. The proposed beating scheme without a need of any moving part in the system has been experimentally proved. The measured results show that the frequency tuning coefficients of the terahertz QCL are 6.1 MHz/0.1 K and 2.7 MHz/mA induced by temperature and drive current, respectively, which have been never revealed by a traditional terahertz FTIR spectrometer. Furthermore, compared to FTIR spectrometers, the laser beating technique shows two unique features, i.e., high spectral precision and fast data acquisition. The proposed setup can be also used for high resolution linewidth measurements of narrow absorption lines and multi-channel terahertz communications.

Funding. National Natural Science Foundation of China (62022084, 61875220, 61927813, 61991430, 62035005); Ministry of Science and Technology of the People's Republic of China (2017YFF0106302); Chinese Academy of Sciences (YJKYYQ20200032, ZDBS-LY-JSC009); Science and Technology Commission of Shanghai Municipality (20XD1424700).

Disclosures. The authors declare no conflicts of interest.

Data availability. Data underlying the results presented in this paper are not publicly available at this time but may be obtained from the authors upon reasonable request.

Supplemental document. See [Supplement 1](#) for supporting content.

References

1. M. Tonouchi, "Cutting-edge terahertz technology," *Nat. Photonics* **1**(2), 97–105 (2007).
2. B. S. Williams, "Terahertz quantum-cascade lasers," *Nat. Photonics* **1**(9), 517–525 (2007).
3. B. M. Fischer, M. Hoffmann, H. Helm, R. Wilk, F. Rutz, T. Kleine-Ostmann, M. Koch, and P. U. Jepsen, "Terahertz time-domain spectroscopy and imaging of artificial RNA," *Opt. Express* **13**(14), 5205–5215 (2005).
4. M. M. Coleman and P. C. Painter, "Fourier transform infrared spectroscopy: probing the structure of multicomponent polymer blends," *Appl. Spectrosc. Rev.* **20**(3-4), 255–346 (1984).
5. M. Van Exter, C. Fattinger, and D. Grischkowsky, "Terahertz time-domain spectroscopy of water vapor," *Opt. Lett.* **14**(20), 1128–1130 (1989).
6. I. C. Ho, X. Guo, and X. C. Zhang, "Design and performance of reflective terahertz air-biased-coherent-detection for time-domain spectroscopy," *Opt. Express* **18**(3), 2872–2883 (2010).
7. <https://www.bruker.com/en/products-and-solutions/infrared-and-raman/ft-ir-research-spectrometers/ifs-125hr-high-resolution-ft-ir-spectrometer.html>.
8. I. Coddington, N. Newbury, and W. Swann, "Dual-comb spectroscopy," *Optica* **3**(4), 414–426 (2016).
9. F. Keilmann, C. Gohle, and R. Holzwarth, "Time-domain mid-infrared frequency-comb spectrometer," *Opt. Lett.* **29**(13), 1542–1544 (2004).
10. P. Giaccari, J.-D. Deschênes, P. Saucier, J. Genest, and P. Tremblay, "Active fourier-transform spectroscopy combining the direct RF beating of two fiber-based mode-locked lasers with a novel referencing method," *Opt. Express* **16**(6), 4347–4365 (2008).
11. M. Yu, Y. Okawachi, A. G. Griffith, N. Picqué, M. Lipson, and A. L. Gaeta, "Silicon-chip-based mid-infrared dual-comb spectroscopy," *Nat. Commun.* **9**(1), 1–6 (2018).
12. Y. Yang, D. Burghoff, D. J. Hayton, J.-R. Gao, J. L. Reno, and Q. Hu, "Terahertz multiheterodyne spectroscopy using laser frequency combs," *Optica* **3**(5), 499–502 (2016).
13. H. Li, Z. Li, W. Wan, K. Zhou, X. Liao, S. Yang, C. Wang, J. Cao, and H. Zeng, "Toward compact and real-time terahertz dual-comb spectroscopy employing a self-detection scheme," *ACS Photonics* **7**(1), 49–56 (2020).
14. L. A. Sterczewski, J. Westberg, Y. Yang, D. Burghoff, J. Reno, Q. Hu, and G. Wysocki, "Terahertz spectroscopy of gas mixtures with dual quantum cascade laser frequency combs," *ACS Photonics* **7**(5), 1082–1087 (2020).

15. L. Consolino, M. Nafa, M. D. Regis, F. Cappelli, K. Garrasi, F. Mezzapesa, L. Li, A. Davies, E. H. Linfield, M. Vitiello, S. Bartalini, and P. D. Natale, "Quantum cascade laser based hybrid dual comb spectrometer," *Commun. Phys.* **3**(1), 69 (2020).
16. Y. Zhao, Z. Li, K. Zhou, X. Liao, W. Guan, W. Wan, S. Yang, J. C. Cao, D. Xu, S. Barbieri, and H. Li, "Phase locking of terahertz semiconductor dual-comb laser sources," *Laser Photonics Rev.* **15**(4), 2000498 (2021).
17. L. Li, L. Chen, J. Freeman, M. Salih, P. Dean, A. Davies, and E. Linfield, "Multi-watt high-power thz frequency quantum cascade lasers," *Electron. Lett.* **53**(12), 799–800 (2017).
18. C. A. Curwen, J. L. Reno, and B. S. Williams, "Terahertz quantum cascade vecsel with watt-level output power," *Appl. Phys. Lett.* **113**(1), 011104 (2018).
19. W. Wan, H. Li, and J. Cao, "Homogeneous spectral broadening of pulsed terahertz quantum cascade lasers by radio frequency modulation," *Opt. Express* **26**(2), 980–989 (2018).
20. G. Scalari, C. Walther, M. Fischer, R. Terazzi, H. Beere, D. Ritchie, and J. Faist, "THz and sub-THz quantum cascade lasers," *Laser Photonics Rev.* **3**(1-2), 45–66 (2009).
21. L. Li, I. Kundu, P. Dean, E. H. Linfield, and A. G. Davies, "High-power GaAs/AlGaAs quantum cascade lasers with emission in the frequency range 4.7-5.6 THz," in *International Quantum Cascade Lasers School & Workshop*, (2016).
22. A. Khalatpour, A. K. Paulsen, C. Deimert, Z. R. Wasilewski, and Q. Hu, "High-power portable terahertz laser systems," *Nat. Photonics* **15**(1), 16–20 (2021).
23. S. Kumar, B. S. Williams, Q. Qin, A. M. Lee, Q. Hu, and J. L. Reno, "Surface-emitting distributed feedback terahertz quantum-cascade lasers in metal-metal waveguides," *Opt. Express* **15**(1), 113–128 (2007).
24. L. Sirigu, R. Terazzi, M. I. Amanti, M. Giovannini, J. Faist, L. A. Dunbar, and R. Houdré, "Terahertz quantum cascade lasers based on two-dimensional photonic crystal resonators," *Opt. Express* **16**(8), 5206–5217 (2008).
25. Y. Chassagneux, R. Colombelli, W. Maineult, S. Barbieri, H. Beere, D. Ritchie, S. Khanna, E. Linfield, and A. G. Davies, "Electrically pumped photonic-crystal terahertz lasers controlled by boundary conditions," *Nature* **457**(7226), 174–178 (2009).
26. G. Xu, Y. Halioua, S. Moudji, R. Colombelli, H. E. Beere, and D. A. Ritchie, "Stable single-mode operation of surface-emitting terahertz lasers with graded photonic heterostructure resonators," *Appl. Phys. Lett.* **102**(23), 231105 (2013).
27. L. Coldren, B. Miller, K. Iga, and J. Rentschler, "Monolithic two-section GaInAsP/InP active-optical-resonator devices formed by reactive ion etching," *Appl. Phys. Lett.* **38**(5), 315–317 (1981).
28. H. Li, J. Manceau, A. Andronico, V. Jagtap, C. Sirtori, L. Li, E. Linfield, A. Davies, and S. Barbieri, "Coupled-cavity terahertz quantum cascade lasers for single mode operation," *Appl. Phys. Lett.* **104**(24), 241102 (2014).
29. Z. Li, H. Li, W. Wan, K. Zhou, and J. Cao, "Sideband generation of coupled-cavity terahertz semiconductor lasers under active radio frequency modulation," *Opt. Express* **26**(25), 32675–32690 (2018).
30. A. W. M. Lee, B. S. Williams, S. Kumar, Q. Hu, and J. L. Reno, "Tunable terahertz quantum cascade lasers with external gratings," *Opt. Lett.* **35**(7), 910–912 (2010).
31. C. A. Curwen, J. L. Reno, and B. S. Williams, "Broadband continuous single-mode tuning of a short-cavity quantum-cascade VECSEL," *Nat. Photonics* **13**(12), 855–859 (2019).
32. R. Lang and K. Kobayashi, "External optical feedback effects on semiconductor injection laser properties," *IEEE J. Quantum Electron.* **16**(3), 347–355 (1980).
33. T. M. Bosch, N. Servagent, and S. Donati, "Optical feedback interferometry for sensing application," *Opt. Eng.* **40**(1), 20–27 (2001).
34. G. Giuliani, S. Bozzi-Pietra, and S. Donati, "Self-mixing laser diode vibrometer," *Meas. Sci. Technol.* **14**(1), 24–32 (2003).
35. R. P. Green, J.-H. Xu, L. Mahler, A. Tredicucci, F. Beltram, G. Giuliani, H. E. Beere, and D. A. Ritchie, "Linewidth enhancement factor of terahertz quantum cascade lasers," *Appl. Phys. Lett.* **92**(7), 071106 (2008).
36. P. Dean, Y. L. Lim, A. Valavanis, R. Kliese, M. Nikolić, S. P. Khanna, M. Lachab, D. Indjin, Z. Ikonić, P. Harrison, A. D. Rakić, E. H. Linfield, and A. G. Davies, "Terahertz imaging through self-mixing in a quantum cascade laser," *Opt. Lett.* **36**(13), 2587–2589 (2011).
37. L. Consolino, S. Jung, A. Campa, M. D. Regis, S. Pal, J. H. Kim, K. Fujita, A. Ito, M. Hitaka, S. Bartalini, P. D. Natale, M. Belkin, and M. Vitiello, "Spectral purity and tunability of terahertz quantum cascade laser sources based on intracavity difference-frequency generation," *Sci. Adv.* **3**(9), e1603317 (2017).
38. M. Rösch, G. Scalari, G. Villares, L. Bosco, M. Beck, and J. Faist, "On-chip, self-detected terahertz dual-comb source," *Appl. Phys. Lett.* **108**(17), 171104 (2016).
39. H. Li, P. Laffaille, D. Gacemi, M. Apfel, C. Sirtori, J. Leonardon, G. Santarelli, M. Rösch, G. Scalari, M. Beck, J. Faist, W. Hänsel, R. Holzwarth, and S. Barbieri, "Dynamics of ultra-broadband terahertz quantum cascade lasers for comb operation," *Opt. Express* **23**(26), 33270–33294 (2015).
40. M. Wienold, L. Schrottke, M. Giehler, R. Hey, W. Anders, and H. Grahm, "Low-threshold terahertz quantum-cascade lasers based on GaAs/Al_{0.25}Ga_{0.75}As heterostructures," *Appl. Phys. Lett.* **97**(7), 071113 (2010).
41. R. A. Mohandas, L. Ponnampalam, L. Li, P. Dean, A. J. Seeds, E. H. Linfield, A. G. Davies, and J. R. Freeman, "Exact frequency and phase control of a terahertz laser," *Optica* **7**(9), 1143–1149 (2020).